

RESEARCH ARTICLE

N-Homocysteinylation Induces Different Structural and Functional Consequences on Acidic and Basic Proteins

Gurumayum Suraj Sharma, Tarun Kumar, Laishram Rajendrakumar Singh*

Dr. B. R. Ambedkar Center for Biomedical Research, University of Delhi, Delhi, India

*lairsingh@gmail.com



OPEN ACCESS

Citation: Sharma GS, Kumar T, Singh LR (2014) N-Homocysteinylation Induces Different Structural and Functional Consequences on Acidic and Basic Proteins. PLoS ONE 9(12): e116386. doi:10.1371/journal.pone.0116386

Editor: Shantanu Sengupta, CSIR-Institute of Genomics and Integrative Biology, India

Received: August 26, 2014

Accepted: December 6, 2014

Published: December 31, 2014

Copyright: © 2014 Sharma et al. This is an open-access article distributed under the terms of the [Creative Commons Attribution License](https://creativecommons.org/licenses/by/4.0/), which permits unrestricted use, distribution, and reproduction in any medium, provided the original author and source are credited.

Data Availability: The authors confirm that all data underlying the findings are fully available without restriction. All relevant data are within the paper and its Supporting Information files.

Funding: The authors have no support or funding to report.

Competing Interests: The authors have declared that no competing interests exist.

Abstract

One of the proposed mechanisms of homocysteine toxicity in human is the modification of proteins by the metabolite of Hcy, homocysteine thiolactone (HTL). Incubation of proteins with HTL has earlier been shown to form covalent adducts with ϵ -amino group of lysine residues of protein (called N-homocysteinylation). It has been believed that protein N-homocysteinylation is the pathological hallmark of cardiovascular and neurodegenerative disorders as homocysteinylation induces structural and functional alterations in proteins. In the present study, reactivity of HTL towards proteins with different physico-chemical properties and hence their structural and functional alterations were studied using different spectroscopic approaches. We found that N-homocysteinylation has opposite consequences on acidic and basic proteins suggesting that pI of the protein determines the extent of homocysteinylation, and the structural and functional consequences due to homocysteinylation. Mechanistically, pI of protein determines the extent of N-homocysteinylation and the associated structural and functional alterations. The study suggests the role of HTL primarily targeting acidic proteins in eliciting its toxicity that could yield mechanistic insights for the associated neurodegeneration.

Introduction

Hyperhomocysteinemia/homocystinuria is a genetic disorder of methionine metabolism caused due to elevated level of plasma homocysteine (Hcy). The toxic Hcy is known to metabolize to methionine by remethylation or to cysteine by trans-sulfurylation. However, mutations in the Hcy metabolizing enzymes, cystathionine β -synthase (CBS) or methylene tetrahydrofolate reductase (MTHFR) cause an impaired ability to metabolize the toxic Hcy resulting in an

increased levels of cellular and plasma Hcy [1, 2, 3, 4, 5]. The total concentrations of plasma Hcy may range from 15–20 μM (mild forms) up to 500 μM (severe forms), compared with 5–10 μM under normal conditions [6, 7, 8, 9, 10, 11]. This elevated Hcy levels are associated with increased incidences of cardiovascular diseases, including atherosclerosis and thrombosis [12, 13], pregnancy disorders [14] and with various neurodegenerative pathologies such as dementia, Parkinson's and Alzheimer's diseases [15, 16, 17]. Indeed, cells have evolved mechanisms for the clearance of this toxic HTL. Urinary excretion of HTL in the kidneys [3, 18] and serum homocysteine-thiolactonase associated with high density lipoprotein which is known to hydrolyse HTL [19], form the extracellular mode of HTL clearance from the body, while bleomycin hydrolase (BHL) is the major intracellular HTL-hydrolysing enzyme which protects the cells against intracellular HTL [20]. However, under severe hyperhomocysteinemic conditions, the effectiveness of these mechanisms in protecting cells against HTL toxicity are still not yet investigated and properly understood.

Several studies have shown that one of the likely mechanisms underlying harmful effects of homocysteine (Hcy) is the chemical modification of protein by homocysteine thiolactone (HTL), a highly reactive cyclic thioester of Hcy [21, 22, 23, 24], which is formed by methionyl-tRNA synthetase [21, 24, 25] in an error editing reaction. It has been demonstrated that HTL preferentially forms amide bonds with ϵ -amino group of protein lysine residues in a non-enzymatic mechanism; a process referred to as “protein N-homocysteinylation” [19]. Protein N-homocysteinylation, has therefore, been considered to be one of the basic causes of HTL toxicity. Incorporation of HTL to the proteins is believed to result in loss of protein functions due to alterations in the protein structure and become susceptible to further damage by oxidation [22, 26, 27]. In addition, it has also been observed in few proteins that N-homocysteinylation induces protein aggregation or amyloid formation and hence considered to be an independent risk factor for neurodegenerative diseases in human [17, 22, 28, 29, 30, 31, 32]. It may be noted that a large fraction of the plasma proteins and many proteins from other sources have been identified for protein N-homocysteinylation both *in vivo* and *in vitro* [22, 33]. However, all the structural and functional based studies have been limited to very few proteins. Since, the total number of proteins modified is large and includes proteins having different physico-chemical properties and fold types, it is important to investigate the structural and functional consequences of HTL on proteins having different physico-chemical properties. In the present study, we have investigated the effects of HTL on three different proteins having different physico-chemical properties (namely lysozyme, RNase-A and alpha-LA). We found that N-homocysteinylation has opposite consequences on acidic and basic proteins suggesting that pI of the protein determines the extent of homocysteinylation, and the structural and functional consequences due to homocysteinylation. Most interestingly, basic proteins are resistant to the structural and functional loss due to N-homocysteinylation indicating that homocysteinylation does not necessarily lead to functional alterations.

Materials and Methods

Materials

Commercially lyophilized preparations of lysozyme (from chicken egg white), ribonuclease-A (RNase-A; from bovine pancreas), alpha-lactalbumin, alpha-casein (α -LA and CN respectively; from bovine milk) and carbonic anhydrase II (CA from bovine erythrocytes) were purchased from Sigma Chemical Co. DL-homocysteine thiolactone hydrochloride, 8-anilino-1-naphthalene sulfonic acid (ANS), thioflavin-T (ThT), 5, 5'-Dithiobis (2-nitrobenzoic acid), cytidine 2'-3' cyclic monophosphate (C>p), *M. luteus* cells and p-nitrophenol acetate (pNPA) were also obtained from Sigma Chemical Co. Potassium chloride and potassium phosphate were obtained from Merck. Guanidinium chloride (GdmCl) was the ultrapure sample from MP Biomedicals. These and other chemicals, which are of analytical grade, were used without further purification.

Lysozyme, RNase-A, α -LA, CN and CA solutions were dialyzed extensively against 0.1 M KCl at pH 7.0 in cold ($\sim 4^{\circ}\text{C}$). Protein stock solutions were filtered using 0.22 μm millipore syringe filters. Concentrations of the protein solutions were determined experimentally using ϵ , the molar extinction coefficient values of 39000 $\text{M}^{-1}\text{cm}^{-1}$ at 280 nm for lysozyme [34], 9800 $\text{M}^{-1}\text{cm}^{-1}$ at 277.5 nm for RNase-A [35], 29210 $\text{M}^{-1}\text{cm}^{-1}$ at 280 nm for α -LA [36], 11,000 $\text{M}^{-1}\text{cm}^{-1}$ at 280 nm for CN [37] and 57,000 $\text{M}^{-1}\text{cm}^{-1}$ at 280 nm for CA [38]. The concentration of GdmCl stock solution was determined by refractive index measurements [39]. All solutions for optical measurements were prepared in the appropriate degassed buffer. All experiments were carried out in 0.05 M potassium phosphate buffer (pH 7.4) containing 0.1 M KCl at 37°C.

Protein N-homocysteinylation

All proteins (2 mg ml^{-1}) were incubated in the presence of different concentrations of HTL (0–1000 μM) in 0.05 M potassium phosphate buffer, pH 7.4 overnight at 37°C. The HTL treated/untreated protein samples were further used for subsequent studies.

Protein sulfhydryl estimation using Ellman's reagent

Protein sulfhydryl (SH) group estimation was carried out as described by Ellman [40] with some minor modifications. Briefly, fractions containing unmodified and modified proteins were solubilized in 6 M guanidinium hydrochloride in presence of 2 mM β -mercaptoethanol (ME) and incubated for 1 h at 37°C as described earlier [30, 31, 32]. Proteins were then precipitated down with 10% TCA to remove unbound HTL. Protein pellets were collected and resolubilized in phosphate buffer, pH 7.0. The levels of thiol groups in control and homocysteinylation protein samples were assayed using 5, 5'-Dithiobis (2-nitrobenzoic acid), the Ellman's reagent [40]. The absorbance of the samples was measured at 412 nm, using a 1 cm path-length cuvette. The amount of 5'-nitrothiobenzoate

released was estimated from the molar extinction coefficient (ϵ) of $13,700 \text{ M}^{-1} \text{ cm}^{-1}$.

Circular Dichroism (CD) Measurements

CD measurements (at least in triplicates) were made in a Jasco J-810 spectropolarimeter equipped with a Peltier-type temperature controller with six accumulations. Protein concentration used for the CD measurements was 0.5 mg ml^{-1} . Cells of 0.1 and 1.0 cm path lengths were used for the measurements of the far- and near-UV CD spectra, respectively. Necessary blanks were subtracted for each measurement. All readings were procured at 37°C . The CD instrument was routinely calibrated with D-10-camphorsulfonic acid. Secondary structure estimation from the far-UV CD spectra was calculated using Yang's method [41].

Fluorescence Measurements

Fluorescence spectra of the protein samples were measured in a Perkin Elmer LS 55 Spectrofluorimeter in a 3 mm quartz cell, with both excitation and emission slits set at 10 nm (at least in triplicates). Protein concentration for all the experiments was $2 \mu\text{M}$ for lysozyme; $5 \mu\text{M}$ for RNase-A, α -LA, CN and CA. For intrinsic fluorescence measurements, RNase-A was excited at 268 nm, while the emission spectra were recorded from 290–350 nm. Lysozyme, α -LA, CN and CA were excited at 295 nm and the emission spectra were recorded in the wavelength region 300–450 nm.

For ANS-protein binding experiments, the excitation wavelength was 360 nm, and emission spectra were recorded from 400–600 nm. ANS concentration was kept 16 fold that of protein concentration. For ThT-protein binding experiments, the excitation wavelength used was 450 nm, and emission spectra were recorded from 475–570 nm. ThT concentration was kept $25 \mu\text{M}$. Necessary blanks were subtracted for each sample. Each spectrum was repeated at least three times.

Transmission electron microscopy

Modified protein solutions were placed on a copper grid and left at room temperature for 5 min. For negative staining of the samples, 1.0% uranyl acetate solution was added on to the copper grid and allowed to air dry before examination using a FEI Tecnai G2-200kV HRTA transmission electron microscopy (Netherlands) operating at 200 kV.

Dynamic light scattering measurements

Size distribution of the particles present in the protein sample were obtained using a Zetasizer Micro V/ZMV 2000 (Malvern, UK). Measurements were made at a fixed angle of 90° using an incident laser beam of 689 nm. Fifteen measurements were made with an acquisition time of 30 seconds for each sample at sensitivity of

10%. The data was analysed using Zetasizer software provided by the manufacturer to get hydrodynamic diameters. The protein concentration was 2.0 mg ml^{-1} . All measurements were performed at 37°C .

Activity measurements

For measuring lysozyme activity, we used *M. luteus* cells as substrate and followed the procedure of Maurel and Douzou [42]. The reaction was followed in Jasco V-660 UV/Visible spectrophotometer. We observed that the apparent specific absorbance (the slope of the straight line obtained by plotting the decrease in absorbance at 450 nm against concentration of the substrate in the range $0\text{--}150 \text{ mg l}^{-1}$) of an aqueous suspension of *M. luteus* cells was $\varepsilon_{450} = 0.65 \times 10^{-2} \text{ mg l}^{-1}$. Just before the initiation of the enzymatic reaction, a given concentration of the substrate in the buffer was transferred to sample and reference cuvettes which was kept at $37.0 \pm 0.1^\circ\text{C}$ and allowed to equilibrate for 15 min. In order to follow the progress curve, $25 \mu\text{l}$ of lysozyme from the stock of 2 mg ml^{-1} was added in the sample cuvette by rapid mixing. To reflect the same dilution, $25 \mu\text{l}$ of buffer was also added in the reference cuvette. The decrease in absorbance, which occurred during the lysis of the cell wall, was recorded at 450 nm for 20 min. The initial velocity (v) of lysis was deduced from the slope of the linear part of the recordings, usually over 30 s. This experiment was repeated for different concentrations of the substrate in the range $10\text{--}150 \text{ mg ml}^{-1}$, and a plot of v versus $[S]$ (in mg l^{-1}) was generated. The plot of v versus $[S]$ was analyzed for K_m and V_{\max} using the relation (Equation 1),

$$v = V_{\max}[S]/(K_m + [S]) \quad (1)$$

where v is the initial velocity, and $[S]$ is the substrate concentration. From this analysis the values of k_{cat} were determined.

In order to see the effect of a HTL on the kinetic parameters (K_m and k_{cat}) of lysozyme, the substrate and the enzyme were pre-incubated in a given concentration of the HTL. Reaction at each concentration of the HTL was followed exactly the same way as described for the control experiment.

Following the procedure described by Crook *et al.* [43], RNase-A activity using cytidine 2'-3' cyclic monophosphate (C>p) as a substrate was measured. Progress curve for RNase-A mediated hydrolysis of C>p in the concentration range ($0.05\text{--}0.50 \text{ mg ml}^{-1}$) in the absence and presence of a given concentration of a HTL was followed by measuring change in absorbance at 292 nm for 20 min in Jasco V-660 UV/Vis spectrophotometer. Sample and reference cells were maintained at $37.0 \pm 0.1^\circ\text{C}$. From each progress curve at a given substrate concentration and in the absence and presence of a fixed HTL concentration, initial velocity (v) was determined from the linear portion of the progress curve, usually 30 s. The plot of initial velocity (v) versus $[S]$ (in mM) at each HTL concentration was analyzed for K_m and k_{cat} using Eq. (1).

Thermal Denaturation Studies

Thermal denaturation studies were carried out in a Jasco V-660 UV/Visible spectrophotometer equipped with a Peltier-type temperature controller at a heating rate of 1 °C per minute. This scan rate was found to provide adequate time for equilibration. Each sample was heated from 37 to 85 °C. The change in absorbance with increasing temperature was followed at 287 nm for RNase-A, 300 nm for lysozyme. About 500 data points of each transition curve were collected. Measurements were repeated three times. After denaturation, the protein sample was immediately cooled down to measure reversibility of the reaction. Each heat-induced transition curve was analyzed for T_m (midpoint of denaturation) using a non-linear least squares method according to the relation (Equation 2),

$$y(T) = \frac{y_N(T) + y_D(T)\exp[-\Delta H_m/R(1/T - 1/T_m)]}{1 + \exp[-\Delta H_m/R(1/T - 1/T_m)]} \quad (2)$$

where $y(T)$ is the optical property at temperature T (Kelvin), $y_N(T)$ and $y_D(T)$ are the optical properties of the native and denatured protein molecules at T K, respectively, and R is the gas constant. In the analysis of the transition curve, it was assumed that a parabolic function describes the dependence of the optical properties of the native and denatured protein molecules (i.e.

$y_N(T) = a_N + b_NT + c_NT^2$ and $y_D(T) = a_D + b_DT + c_DT^2$, where a_N , b_N , c_N , a_D , b_D , and c_D are temperature-independent coefficients) [44].

Results

To investigate the effects of N-homocysteinylation on proteins, we have chosen lysozyme, RNase-A and α -LA. The choice of the proteins was to have different isoelectric points (pI) and fold types keeping in mind that the proteins should also have different lysine contents (See Table 1). To modify proteins by HTL, each of the protein samples (2 mg ml⁻¹) was treated with different concentrations of HTL, ranging from 0–1000 μ M (incubated overnight at pH 7.4) and analyzed for the free SH contents using Ellman's reagent (See Table 2). HTL has been shown to be quite stable at room temperature with less than 10% degradation after 24 hours under physiological conditions [18, 21, 45, 46, 47, 48]. Hence, overnight (12–15 hrs) incubations would thereby lead to minimal hydrolysis of HTL. It is seen in Table 2 that the proteins have been incorporated with HTL as suggested by large increase in the free SH contents. Fig. 1 shows far-UV CD (left panel) and near-UV CD (right panel) spectra of the three HTL-modified proteins. This figure indicates that HTL-induced modification has different structural consequences on α -LA relative to lysozyme and RNase-A, in terms of secondary (far-UV CD) and tertiary (near-UV CD) structures. We further confirmed the alterations in the tertiary structure of the proteins due to the modification by measuring tryptophan/tyrosine fluorescence spectra of the homocysteinyalated proteins. Fig. 2 (left panel) shows representative tryptophan/tyrosine fluorescence spectra

Table 1. Characteristics of lysozyme, RNase-A, α -LA, CN and CA.

	Lysozyme	RNase-A	α -LA	CN	CA
Molecular weight (kDa)	14.3	13.7	14.2	23	29
Number of Amino acids	129	124	123	214	260
pI	11.3	9.6	4.5	4.2	5.9
Fold type	α	$\alpha\beta$	α	IDP*	β
Secondary Structure (%)					
α -helix	30	21	26	18	21
β -sheet	13	39	15	26	36
No. of lysine residues	6	10	12	14	18

* The abbreviation of IDP is intrinsically disordered protein.

doi:10.1371/journal.pone.0116386.t001

of the modified and unmodified proteins and the right panel shows the observed fluorescence maxima (F_{max}) at different concentrations of HTL.

We then performed ANS and ThT binding assays to investigate if N-homocysteinylation induces aggregate formation of the HTL-modified proteins (Fig. 3 and Fig. 4). It was observed that there is no binding of both ANS and ThT in case of lysozyme and RNase-A at different concentrations of HTL, as neither the λ_{max} was blue shifted (for ANS) nor there is an increase in the relative fluorescence intensities for both ANS and ThT. Whereas in the case of α -LA there is an increase in both the ANS and ThT binding in an HTL concentration dependent manner upon modification by HTL indicating the presence of protein aggregates that might be amyloidogenic. Transmission electron microscopy images (Fig. 5) further confirm that N-homocysteinylation-induced aggregates in α -LA are not amyloidogenic in nature. S1 Fig. shows the size distribution by volume and Table 3 shows the hydrodynamic diameter of protein aggregates obtained from DLS measurements. It is seen in S1 Fig. that there is existence of large aggregates due to modification. The results together indicate that protein

Table 2. Protein free sulfhydryl contents on modification by HTL.^{a,b}

HTL (μ M)	Lysozyme	RNase-A	α -LA
0	35.78	34.66	36.91
50	45.78	68.48	79.16
100	72.02	91.19	203.65
200	103.31	115.45	325.84
400	163.82	204.16	515.62
600	278.82	331.21	597.19
800	422.86	475.39	833.15
1000	547.74	609.27	935.56

^aErrors sulfhydryl contents are 5–8%.

^bUnit of sulfhydryl contents is (μ M mg^{-1}).

doi:10.1371/journal.pone.0116386.t002

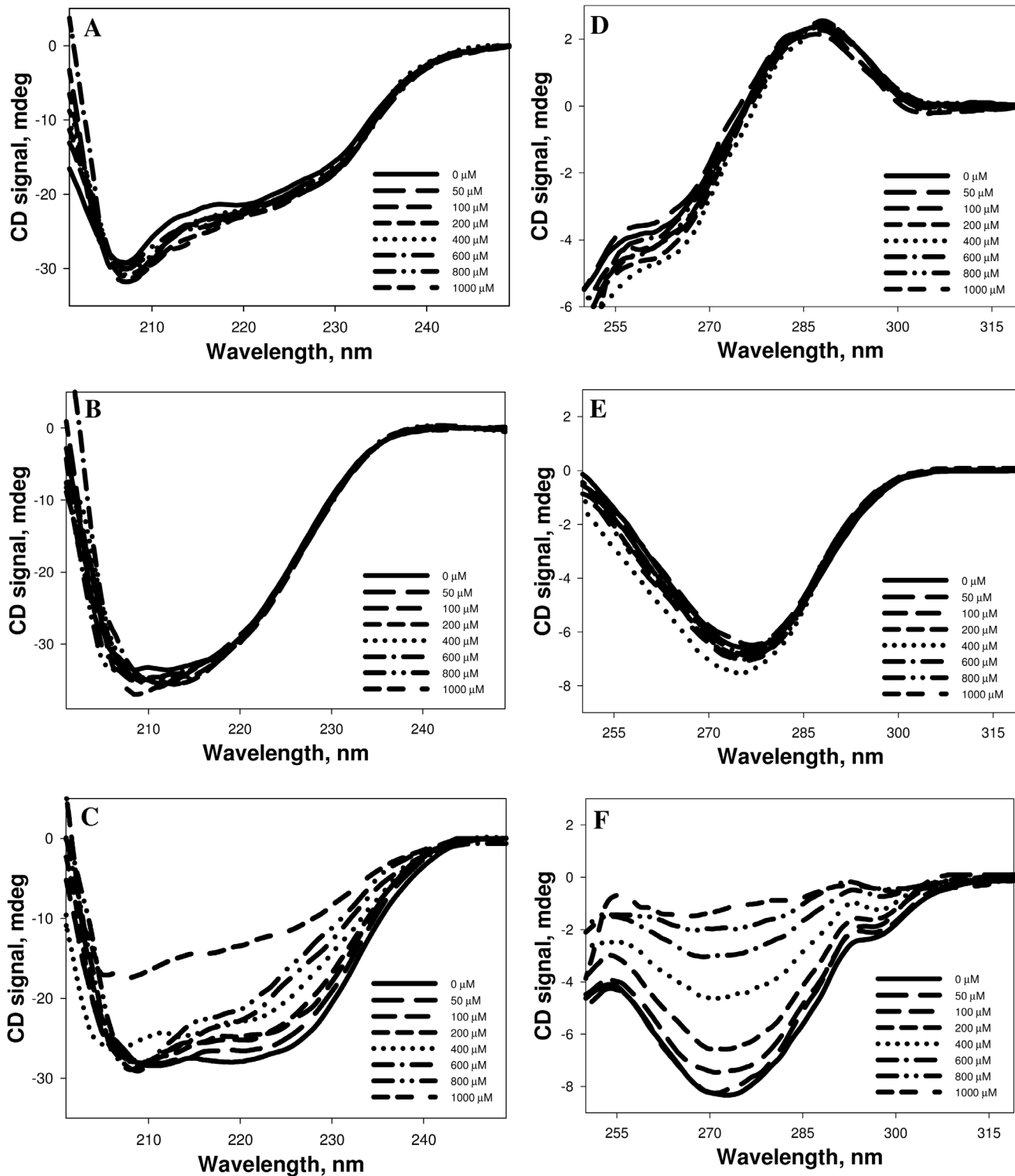


Fig. 1. Circular dichroism spectra of homocysteinylation of proteins. Far-UV CD spectra (at 37°C) of lysozyme (A), RNase-A (B) and α -LA (C) modified with varying concentrations of HTL ranging from 0–1000 μ M, at pH 7.4 (left panel). Near-UV CD spectra of lysozyme (D), RNase-A (E) and α -LA (F) modified with varying concentrations of HTL ranging from 0–1000 μ M, at pH 7.4 (right panel).

doi:10.1371/journal.pone.0116386.g001

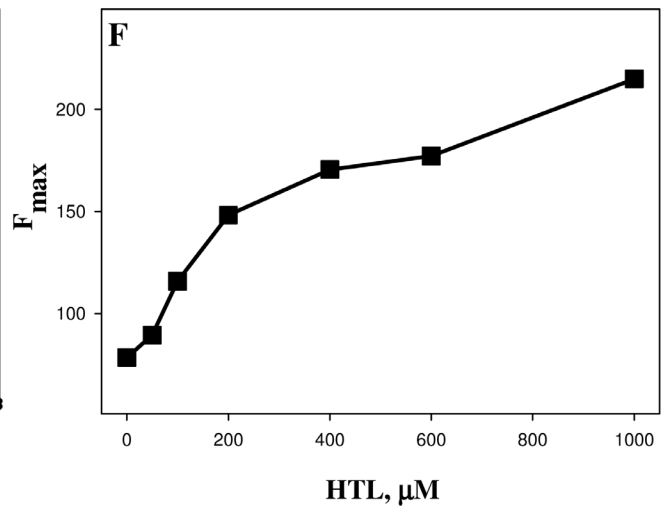
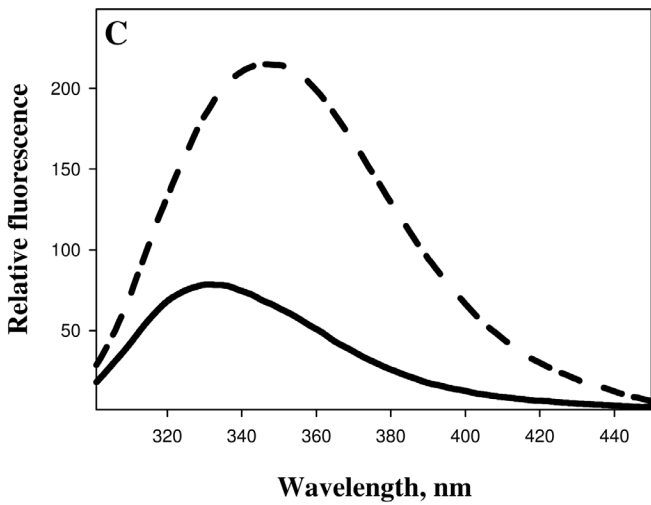
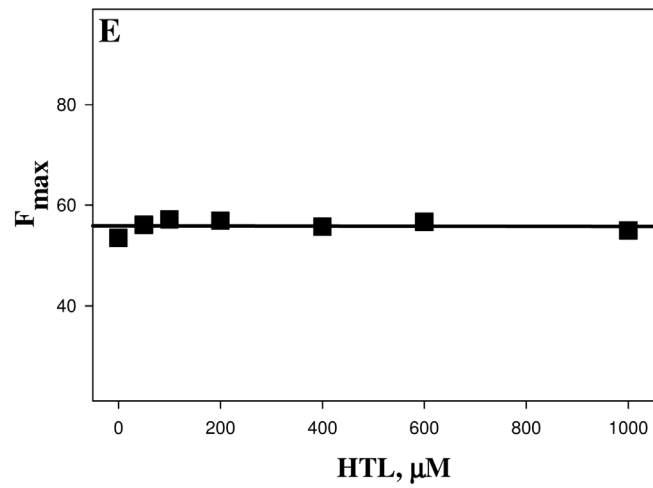
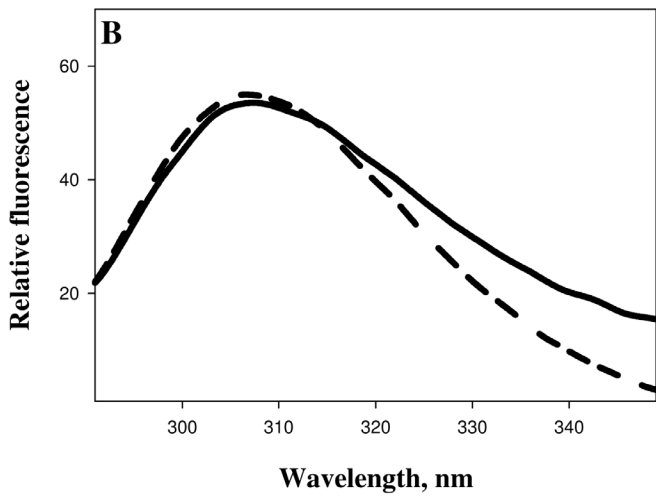
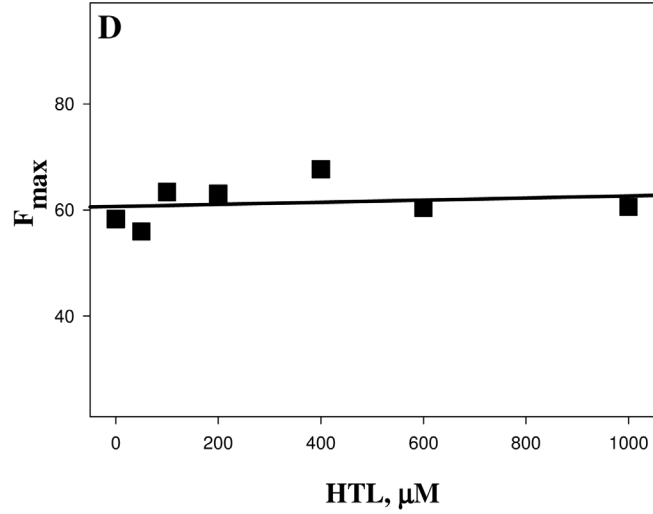
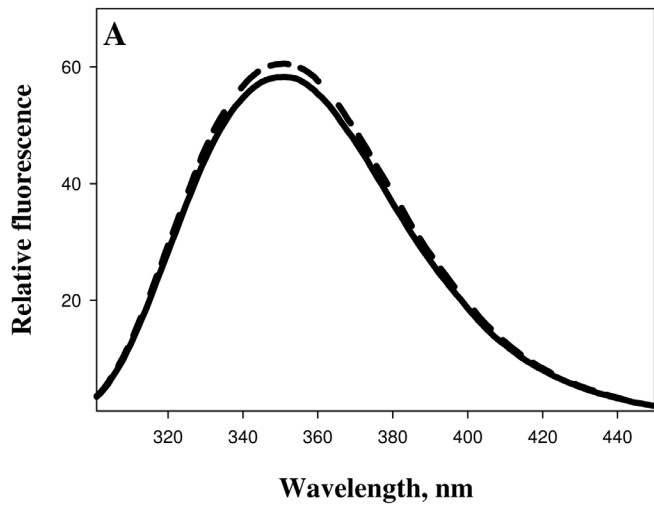


Fig. 2. Intrinsic fluorescence spectra (left panel) of lysozyme (A), RNase-A (B) and α -LA (C) modified with HTL. To maintain clarity, only the representative curves of control unmodified protein (solid lines) and protein modified with 1000 μ M HTL (dashed lines) are shown. Plots of the fluorescence maxima (F_{\max}) as a function of HTL concentrations of lysozyme (D), RNase-A (E) and α -LA (F) are given in the right panel.

doi:10.1371/journal.pone.0116386.g002

covalent modification by N-homocysteinylation has different consequences in terms of structure and aggregation propensities on different proteins.

Following the procedure described in the preceding section, functional activity parameters (K_m and k_{cat}) of lysozyme and RNase-A were measured in the absence and presence of different concentrations of HTL at pH 7.4 and 37°C. [Table 4](#) shows the enzyme kinetic parameters of HTL-modified (and -unmodified) lysozyme and RNase-A. It is seen in this table that there is no significant effect on the functional activity parameters (K_m and k_{cat}) of lysozyme and RNase-A due to the modification. No changes in the K_m and k_{cat} might possibly be due to no effects in the thermodynamic stability of the modified proteins. To uncover this possibility, we performed heat-induced denaturation studies of the modified lysozyme and RNase-A by monitoring the changes in absorbance at 300 nm for lysozyme and 287 nm for RNase-A as a function of temperature. The denaturation profiles are shown in [S3 Fig.](#) and the measured thermodynamic parameter (T_m) are presented in [Table 5](#). It should however be noted that a complete transition curve could not be obtained in the temperature range of 37°C–85°C in the case of lysozyme. Therefore, in order to bring down transition curves in the measurable temperature range, 1.5 M GdmCl was added to the samples in case of lysozyme. Therefore, the transition curves shown in [S3 Fig.](#) for lysozyme (upper panel) is the curve obtained in the presence of 1.5 M GdmCl. The unfolding profiles are given in [S3 Fig.](#) and the evaluated T_m using appropriate equation ([Equation 2](#), see [materials and methods](#)) are given in [Table 5](#). It is seen in [S3 Fig.](#) (and [Table 5](#), for T_m), that there is no significant change in protein stability in terms of T_m . Our results clearly indicate that N-homocysteinylation brought about by HTL does not affect the functional activities of lysozyme and RNase-A by not affecting the thermodynamic stability, T_m .

Discussion

It has been previously reported that protein N-homocysteinylation basically targets the free amino group of lysine residues in protein. Therefore, first of all we have investigated if there is any difference in the extent of homocysteinylation among the proteins (lysozyme, RNase-A and α -LA) having different lysine residues (see [Table 1](#)). The HTL concentrations (0–1000 μ M) used in the present study have been selected keeping in mind that these also represent a near pathological concentrations of Hcy found in severe homocysteinuric conditions [[7](#), [8](#), [9](#), [10](#), [11](#)]. Covalent adduct formation between HTL and protein lysine residues results in the availability of a free SH in the modified protein. Since for each HTL molecule reacting with the free amino group of the protein, an SH

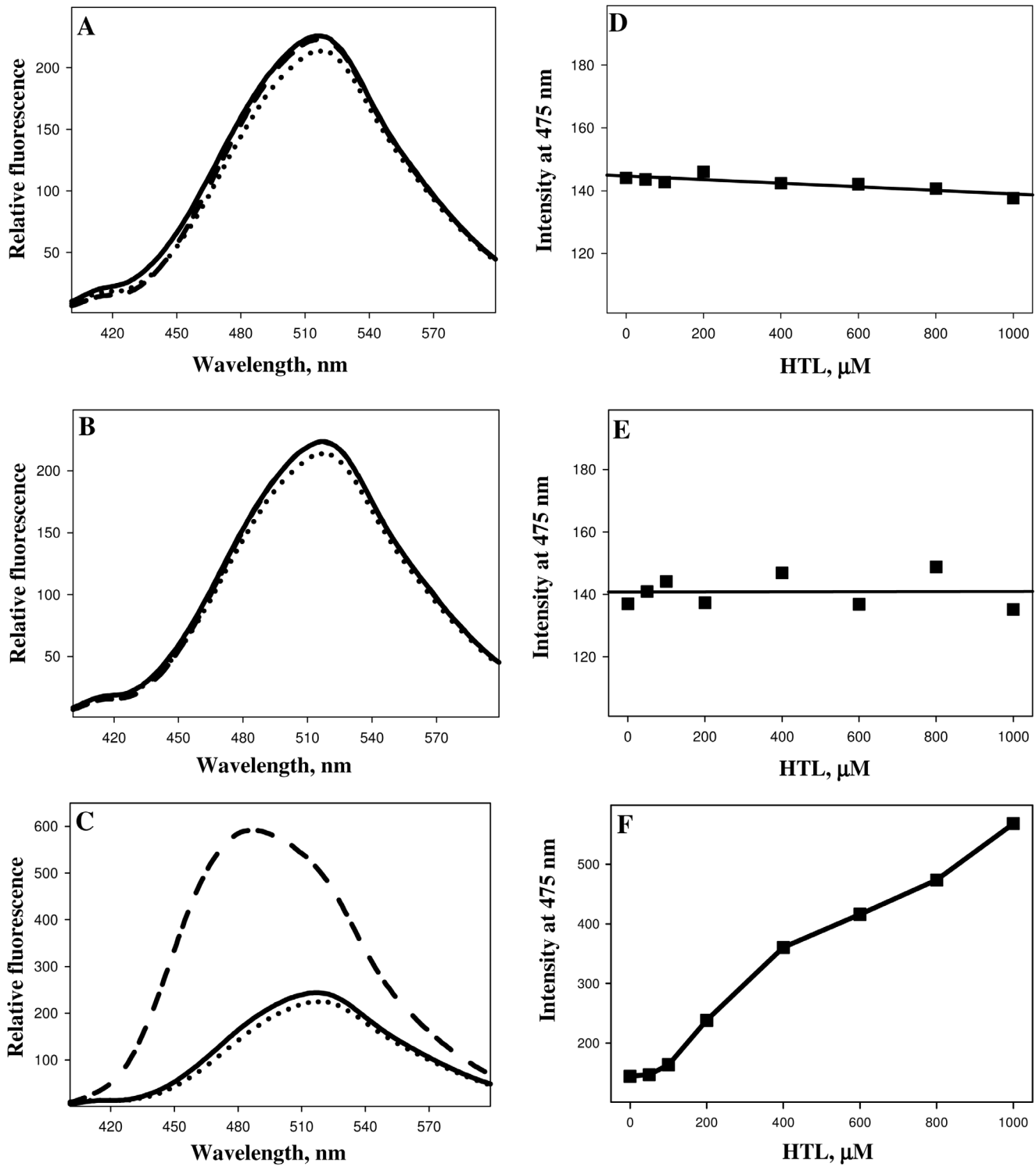


Fig. 3. ANS binding assay (left panel) of lysozyme (A), RNase-A (B) and α -LA (C) treated overnight at 37°C with varying concentrations of HTL. Right panels depict λ_{max} as a function of HTL concentrations of lysozyme (D), RNase-A (E) and α -LA (F). To maintain clarity, only the representative curves of free dyes (dotted lines), control unmodified protein (solid lines) and protein modified with 1000 μ M HTL (dashed lines) are shown.

doi:10.1371/journal.pone.0116386.g003

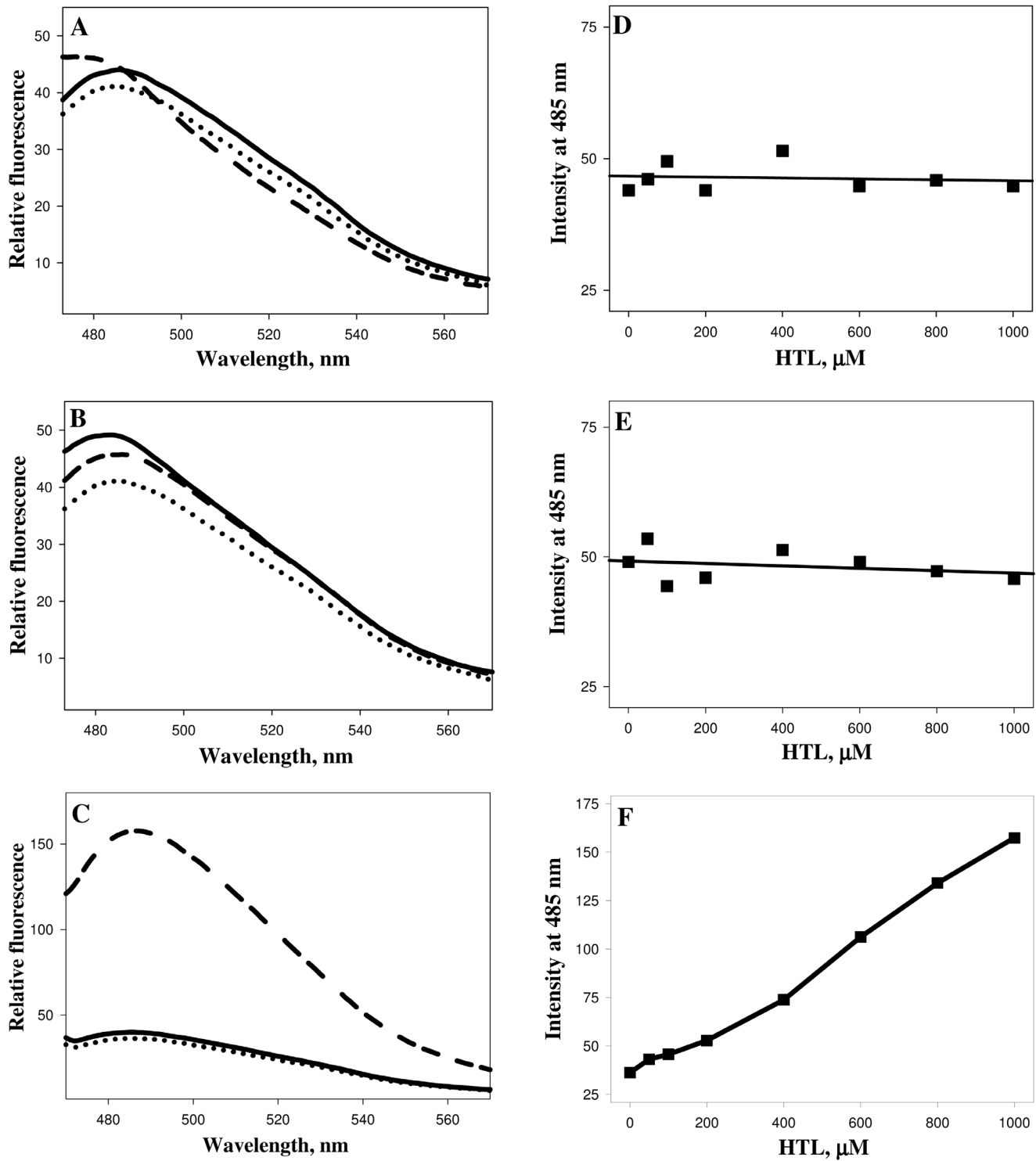


Fig. 4. ThT binding assay (left panel) of lysozyme (A), RNase-A (B) and α -LA (C) treated overnight at 37°C with varying concentrations of HTL. Right panels depict λ_{max} as a function of HTL concentrations of lysozyme (D), RNase-A (E) and α -LA (F). To maintain clarity, only the representative curves of free dyes (dotted lines), control unmodified protein (solid lines) and protein modified with 1000 μM HTL (dashed lines) are shown.

doi:10.1371/journal.pone.0116386.g004

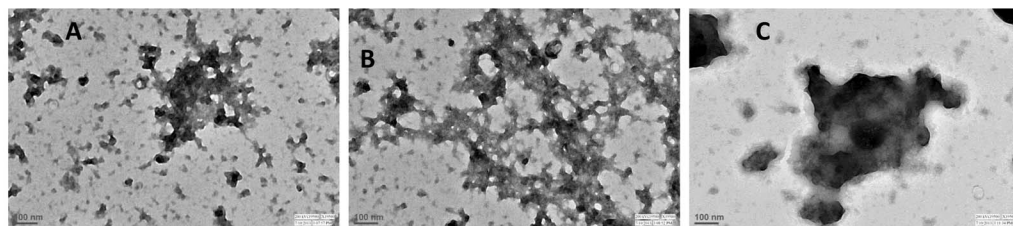


Fig. 5. Transmission electron micrographs of α -LA. Micrographs of α -LA samples incubated overnight with HTL at 37°C (A-400 μ M, B-600 μ M and C-1000 μ M HTL). See also [S1 Fig](#).

doi:10.1371/journal.pone.0116386.g005

group is added which can be assessed using Ellman’s reagent. Hence increase in the free SH content upon HTL treatment is regarded to be a good signature of protein covalent adduct formation by HTL. It is seen in [Table 2](#) that there is an increase in the free SH content of the proteins in a HTL concentration manner suggesting that the proteins have been incorporated with HTL. Interestingly, the extent of homocysteinylation is almost same in the case of lysozyme and RNase-A, but is highest in case of α -LA ([Fig. 6](#)). In terms of number of lysine residues present in the proteins, RNase-A and α -LA should have almost the similar extents of homocysteinylation (as the number of lysine content does not vary much, RNase-A and α -LA have 10 and 12 lysine residues respectively); while lysozyme and RNase-A should have different extent of homocysteinylation as the number of lysine content in RNase-A is relatively higher (See [Table 1](#)). In fact, the dependence of the extent of homocysteinylation on the number of lysine content in proteins has been challenged by several studies [[28](#), [30](#), [49](#), [50](#)]. Since, both lysozyme and RNase-A are basic proteins with close pI values and α -LA is an acidic protein (See [Table 1](#)), we speculated that the differential behaviour of N-homocysteinylation may most probably be due to the differences in their pI values (or the acidic or basic nature) of the proteins. Several serum proteins have been found to have modified with HTL and their rate of N-linked modification due to HTL has also been reported [[22](#)]. It may be noted that most serum proteins

Table 3. Hydrodynamic diameter of HTL-treated α -LA samples.

HTL (μ M)	Hydrodynamic diameter (nm)
0	3.6 \pm .3
50	10.6 \pm .8
100	36.3 \pm 1.5
200	107.9 \pm 8.7, 389.8 \pm 17.9
400	155.7 \pm 8.9, 342.8 \pm 39.6
600	198.3 \pm 10.3, 941.7 \pm 78.3
800	225.6 \pm 23.2, 1044.0 \pm 65.5
1000	428.3 \pm 34.1, 1491.0 \pm 163.4

Solution containing 2 mg ml⁻¹ of α -LA was withdrawn from the reaction mixtures and analysed without any dilution. All measurements were performed at 37°C. The values reported represent the mean \pm SD calculated from three independent experiments.

doi:10.1371/journal.pone.0116386.t003

Table 4. Enzymatic activity parameters (K_m and k_{cat}) of lysozyme and RNase-A treated with different concentrations of HTL^a.

HTL (μM)	Lysozyme		RNase-A	
	K_m ($\mu\text{g ml}^{-1}$)	k_{cat} ($\text{mg ml}^{-1} \text{s}^{-1} \text{M}^{-1}$)	K_m (mM)	k_{cat} (min^{-1})
0	77.8 \pm 2	484.1 \pm 29	1.29 \pm 0.11	191 \pm 22
50	76.9 \pm 4	489.3 \pm 25	1.33 \pm 0.17	185 \pm 23
100	78.1 \pm 3	479.9 \pm 27	1.27 \pm 0.09	192 \pm 25
200	77.4 \pm 4	481.3 \pm 31	1.28 \pm 0.13	195 \pm 28
400	77.6 \pm 3	478.8 \pm 26	1.29 \pm 0.12	194 \pm 23
600	77.1 \pm 2	482.3 \pm 24	1.31 \pm 0.14	196 \pm 27
800	78.3 \pm 3	484.5 \pm 28	1.32 \pm 0.16	189 \pm 22
1000	77.3 \pm 4	481.2 \pm 31	1.25 \pm 0.13	198 \pm 24

^a \pm represents the average errors of three independent measurements.

doi:10.1371/journal.pone.0116386.t004

reported for N-linked homocysteinylation were found to have low pI values. In order to see if pI values might play a role in the N-homocysteinylation of proteins, we have plotted the rate of homocysteinylation as a function of pI for all the serum proteins reported to have modified by homocysteinylation (Fig. 7). Fig. 7 shows that there is a close relation between the pI and the rate of homocysteinylation (k). The existence of such a close relation between the pI and the k values led us to believe that the acidic proteins are prone to N-homocysteinylation while basic proteins tend to have lesser extent of homocysteinylation.

It has been known that protein N-homocysteinylation results in native state structural alterations, loss of enzyme functions and induces protein aggregation/amyloidogenesis [11, 22, 28, 29, 30, 31, 32, 51, 52, 53]. Therefore, it is important to investigate if these consequences of protein homocysteinylation depend on the acidic or basic nature of the proteins. In this spirit, we have investigated if acidic and basic proteins behave differently on being modified by N-homocysteinylation. We have investigated if any difference in the native state conformational changes due to homocysteinylation is responsible for the differential behavior of

Table 5. Melting temperature (T_m) of lysozyme and RNase-A on being treated overnight with HTL at 37°C^a.

HTL (μM)	Lysozyme	RNase-A
0	67.6	63.4
50	67.4	63.5
100	67.8	63.1
200	68.1	63.4
400	68.3	63.3
600	67.6	63.4
800	67.1	62.9
1000	67.3	63.1

^aErrors in T_m are .2–1%. Measurements were repeated at least three times.

doi:10.1371/journal.pone.0116386.t005

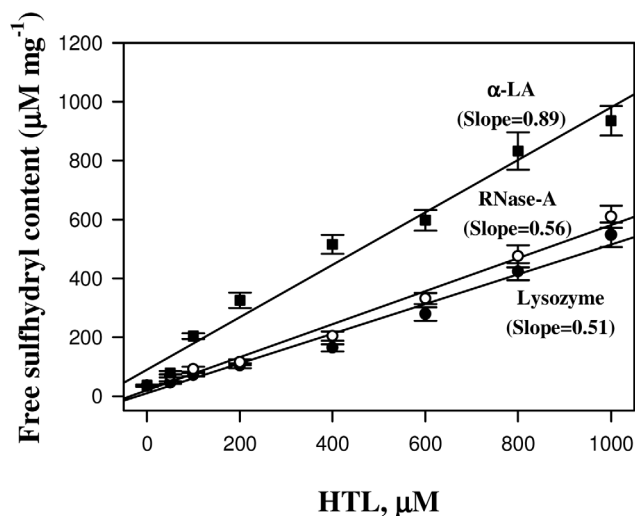


Fig. 6. A comparative analysis for the extent of N-homocysteinylation as assessed by protein free sulfhydryl estimation using Ellman's reagent. Filled circles, open circles and filled squares represent lysozyme, RNase-A and α -LA, respectively.

doi:10.1371/journal.pone.0116386.g006

homocysteinylation on the proteins. For this, we have measured the far-UV, near-UV CD and intrinsic fluorescence spectra of the homocysteinylation proteins. It is seen in Fig. 1 that the secondary structural contents of lysozyme and RNase-A are not changed due to the modification at different concentrations of HTL. In contrast, the secondary structure of α -LA has been reduced significantly in a HTL concentration dependent manner and completely denatured at the highest

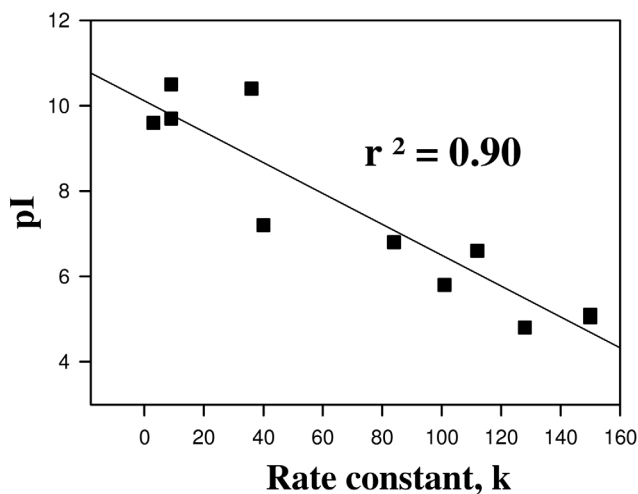


Fig. 7. Relationship between proteins pI and second-order rate constants (k) of their modification by HTL. Second-order rate constants (k) are plotted as a function of the pI for the following proteins: low density lipoproteins, transferrin, albumin, γ -globulin, fibrinogen, hemoglobin, myoglobin, cytochrome c, α -crystallin, trypsin, DNase-I and RNase-A (in order of increasing pI). Values are taken from 22.

doi:10.1371/journal.pone.0116386.g007

Table 6. Percent secondary structure of lysozyme, RNase A and α -LA on modification by HTL.

HTL (μ M)	Lysozyme		RNase-A		α -LA	
	α -helix	β -sheet	α -helix	β -sheet	α -helix	β -sheet
0	27.8	14.6	20.6	40.6	28.9	13.9
50	27.3	13.8	21.1	42.1	27.1	16.2
100	28.6	12.6	19.7	41.6	22.8	18.8
200	28.7	14.1	20.2	42.5	21.5	20.7
400	29.2	14.4	19.8	39.3	16.0	28.3
600	27.9	13.8	19.1	41.7	15.3	30.7
800	29.4	15.1	21.7	40.9	13.7	32.9
1000	28.7	14.8	20.6	40.5	11.3	36.4

Secondary structure estimation was accomplished according to Yang's method (41).

doi:10.1371/journal.pone.0116386.t006

concentration of HTL (1000 μ M). Evaluated percent secondary structural changes (see [Table 6](#)) also suggest that there is no alterations in alpha and beta content of lysozyme and RNase-A samples treated with HTL. However, in the case of α -LA, we observed a decrease in the percent alpha helical content and a concomitant increase in the percent beta sheet structural composition. Thus, N-linked modification of α -LA by HTL brings about structural transition from an alpha to beta sheets but this conversion is absent in the case of lysozyme and RNase-A. Near-UV CD and intrinsic fluorescence spectral measurements of the modified lysozyme and RNase-A at different HTL concentrations also indicate that there is no tertiary structural change due to modification. In case of α -LA, HTL binding induces alterations in the tertiary structure leading to complete loss of tertiary structure at the highest concentration of HTL. In addition to lysozyme and RNase-A used in the present study, many proteins have earlier been reported to be N-homocysteinylation but do not result in structural alterations [49, 51]. Conformational measurements therefore indicate that the differential extent of N-homocysteinylation on acidic (α -LA) and basic (lysozyme and RNase-A) proteins is due to the different effects on the native states of the proteins. At present, we have no concrete explanation for the different effects of HTL-induced modifications on the native states of different proteins. It might, however be possible that disruption of the tertiary contacts due to N-homocysteinylation might be limiting step as the tertiary structures of both lysozyme and RNase-A could not be disrupted due to the modification. Perhaps the incorporation of HTL to specific lysine residues in different proteins might be responsible for the opening of the tertiary structure which in case of α -LA is easily accessible while it is difficult to target in case of lysozyme and RNase-A. In support of our argument, it has been previously reported in cytochrome c (cyt c), that modification of four lysine residues (Lys8 or -13, Lys86 or -87, Lys99, and Lys100) does not bring about any significant change in its native state tertiary structure [49]. However, a single residue modification in case of insulin results in denaturation, ultimately leading to aggregate formation [28, 54]. In addition, different reactivities of lysine

residues in hemoglobin toward HTL were observed in another study [50]. Furthermore, it has been shown that Lys525 is a predominant site of *N*-homocysteinylation in case of human serum albumin and the status of Cys34 determines the reactivity of albumin lysine residues, including Lys525 [55]. All these results provide clear evidence that modification of specific lysine residues is responsible for the observed structural and hence functional consequences.

We have further investigated if all of the homocysteinylation proteins used in this study undergo aggregate formations. For this purpose we analysed the homocysteinylation proteins for ANS and ThT binding propensities. The absence of ANS and ThT binding in lysozyme and RNase-A indicate no possibility of the presence of aggregates in the protein samples treated with HTL. Interestingly the extensively homocysteinylation protein, α -LA (as compared to lysozyme and RNase-A) was found to have a very prominent binding of both ANS and ThT indicating the presence of non-native aggregates which might be most probably amyloids. In addition, DLS measurement suggests the presence of at least two different aggregate species at concentration of HTL beyond 100 μ M (Table 3). On being modified with HTL the hydrodynamic diameter of α -LA is highly increased with predominant particle size of \sim 1500 nm (at 1000 μ M) as compared to 3.56 nm of the control native proteins suggesting that at this concentration of HTL, the monomeric native α -LA has completely disappeared. To further confirm if the aggregates formed are amyloidogenic in nature, we have analyzed them using transmission electron microscopy, which revealed the presence of amorphous structures but not fibrils. Binding of ThT, but absence of fibrils/amyloids might possibly mean that the native α -LA has changed from its alpha helical conformation to predominant beta rich conformations that do not have the propensity to form fibrils. It may be noted that the HTL-induced amyloid formation has so far been reported only on very few proteins [30, 32]. Hence *N*-homocysteinylation-induced amyloid transformation might not be a general consequence on all proteins.

To examine the generality of the dependence of HTL-induced structural alterations on acidic proteins, we performed similar measurements on two additional acidic proteins (α -casein, CN, pI 4.2 and carbonic anhydrase, CA, pI 5.9). Similar to α -LA, it was also found that HTL induces structural alterations in CN and CA, as evident from the changes in the intrinsic fluorescence emission maxima on being treated with HTL and binding of ANS and ThT (See Figs. S2, S4). In agreement to the observed aggregate formation on α -LA, CN and CA, many acidic proteins have been reported to form large oligomers to aggregates upon modification by HTL [28, 29, 30, 32, 52]. Thus it is clear from the results that in contrast to the observed effect on the basic proteins (lysozyme and RNase-A), *N*-homocysteinylation acidic proteins are unfolded leading to aggregate formation.

We have further investigated the effect of *N*-homocysteinylation on the functional activity of the two basic proteins (lysozyme and RNase-A). For this, we carried out measurement of enzymatic kinetic parameters (K_m and k_{cat}) of HTL-modified lysozyme and RNase-A (see Table 4). It should be noted that the value for each kinetic parameter given in Table 4 represents the mean of three

independent measurements and \pm represent the mean error. The kinetic parameters in the absence of the HTL, shown in [Table 4](#), are in excellent agreement with the previous reports [[42](#), [43](#)]. This agreement led us to believe that our measurements of the enzyme-catalyzed reactions and the analysis of the progress curves for kinetic parameters are accurate and authentic. Interestingly, it is also seen in [Table 4](#) that the K_m and k_{cat} of the homocysteinylation of lysozyme and RNase-A are not altered significantly due to N-homocysteinylation suggesting that the enzyme activity is not changed. However, in the case of CA which is an acidic protein, at 1000 μ M HTL concentration, there was almost complete loss of enzyme activity (see [S5 Fig.](#)). No alterations in the thermodynamic stability (in terms of T_m , see [S3 Fig.](#) and [Table 5](#)) due to homocysteinylation in lysozyme and RNase-A further support the fact that the protein functional activity should not be perturbed as protein stability and activity has a direct relation. It is now important to highlight that the commonly held belief of the loss of enzyme activity due to homocysteinylation has been derived from availability of large amount of N-homocysteinylation protein in serum of homocysteinuric patients and the existence of antibodies against these protein adducts, but not based on direct enzymatic activity measurements. However, based on systematic activity measurements, at least four proteins (namely NOS: nitric oxide synthase, MetRS: methionyl-tRNA synthetase, DDAH: dimethylarginine dimethylaminohydrolase and paroxonase) have been reported to result in loss of enzyme activity due to homocysteinylation [[22](#), [51](#), [53](#), [56](#), [57](#)]. All of these proteins reported were found to be acidic in nature with pI values ranging from 5.1–6.2. Thus considering all previous reports and this study, we conclude that N-homocysteinylation-induced protein modifications might be pI dependent, with acidic proteins having higher propensities for structural and functional alterations as compared to basic proteins.

Misfolded protein aggregates and plaques in neuronal cells are emblematic signature of most of the neurological disorders and can trigger cascade of events ultimately resulting in synaptic dysfunction and consequent neuronal death with devastating clinical consequences, and one of the basic symptoms of increased levels of Hcy is neurodegeneration. It is important to note that almost all cytoskeletal proteins are acidic in nature. The possibility of these cytoskeletal proteins getting homocysteinylation is quite high, resulting in loss of their structure and function. This will eventually hamper intracellular transport and trafficking systems, thereby resulting in reduced/loss of neuronal activity. To date, at least two proteins of cytoskeletal origin (microtubule-associated tau protein, neuronal and glial intermediate filaments, IF) [[58](#)] have been reported to be affected by increased level of Hcy. N-homocysteinylation of tau protein has been shown to result in altered tubulin assembly dynamics *in vitro* [[59](#)]. These results clearly indicate that cells or tissues rich in acidic proteins could be the major targets for Hcy induced cytotoxicity and hence a prime cause of neurodegeneration. Taken together, we conclude that N-homocysteinylation-induced loss of protein functions is not generally true and may depend on the physico-chemical properties of the proteins.

Conclusions

We provide here for the first time that the structural and functional consequences due to N-homocysteinylation depend on pI of the proteins. Basic proteins are resistant to structural and functional alterations due to N-homocysteinylation, whereas acidic proteins result in denaturation and ultimately leading to aggregation. The study indicates that not all proteins are prone to HTL-induced structural and functional modifications. In addition, cells or tissues rich in acidic proteins could be the major targets for Hcy-induced cytotoxicity.

Supporting Information

S1 Fig. DLS analysis of both untreated and HTL-treated α -LA sample. Size distribution by volume of control untreated sample (upper panel) and α -LA treated with 1000 μ M HTL (lower panel).

[doi:10.1371/journal.pone.0116386.s001](https://doi.org/10.1371/journal.pone.0116386.s001) (TIF)

S2 Fig. Fluorescence spectra of CN modified with varying concentrations of HTL. Left panel depicts intrinsic fluorescence (A), ANS binding assay (B) and ThT binding assay (C). Right panel depicts F_{\max} as a function of HTL concentration (D), and λ_{\max} as a function of HTL concentrations (E and F). To maintain clarity, only the representative curves of free dyes (dotted lines), control unmodified protein (solid lines) and protein modified with 1000 μ M HTL (dashed lines) are shown.

[doi:10.1371/journal.pone.0116386.s002](https://doi.org/10.1371/journal.pone.0116386.s002) (TIF)

S3 Fig. Representative thermal denaturation profiles of lysozyme and RNase-A. Denaturation curves of lysozyme (upper panel) and RNase-A (lower panel), in the absence and presence of various HTL concentrations at pH 7.4 phosphate buffer.

[doi:10.1371/journal.pone.0116386.s003](https://doi.org/10.1371/journal.pone.0116386.s003) (TIF)

S4 Fig. CD and fluorescence spectra of HTL-modified CA. Far UV-CD (A), intrinsic fluorescence spectra (B), ANS binding assay (C) and D-ThT binding assay (D) of HTL-modified CA. All spectra have been made in absence (solid lines) and in presence of 1000 μ M HTL (dashed lines). In case of ANS and ThT binding assays, free dyes (dotted lines) have also been shown.

[doi:10.1371/journal.pone.0116386.s004](https://doi.org/10.1371/journal.pone.0116386.s004) (TIF)

S5 Fig. Effect of HTL-induced modification on CA enzymatic activity. Enzyme activity (in percent) was measured by monitoring the hydrolysis of p-nitrophenyl acetate (pNPA) at 400 nm. The enzyme concentration used was 0.03 mg ml⁻¹ and substrate was kept 1 mM.

[doi:10.1371/journal.pone.0116386.s005](https://doi.org/10.1371/journal.pone.0116386.s005) (TIF)

Author Contributions

Conceived and designed the experiments: LRS. Performed the experiments: GSS TK. Analyzed the data: LRS GSS TK. Contributed reagents/materials/analysis tools: LRS. Wrote the paper: LRS.

References

1. **Jakubowski H** (1991) Proofreading in vivo: editing of homocysteine by methionyl-tRNA synthetase in the yeast *Saccharomyces cerevisiae*. *EMBO J* 10: 593–598.
2. **Jakubowski H** (2002) The determination of homocysteine-thiolactone in biological samples. *Anal Biochem* 308: 112–119.
3. **Jakubowski H** (2006) Pathophysiological consequences of homocysteine excess. *J Nutr* 136: 1741–1749.
4. **Jakubowski H** (2007) The molecular basis of homocysteine thiolactone-mediated vascular disease. *Clin Chem Lab Med* 45: 1704–1716.
5. **Pancharuniti N, Lewis CA, Sauberlich HE, Perkins LL, Go RC, et al.** (1994) Plasma homocyst(e)ine, folate, and vitamin B-12 concentrations and risk for early-onset coronary artery disease. *Am J Clin Nutr* 59: 940–948.
6. **Gellekink H, den Heijer M, Heil SG, Blom HJ** (2005) Genetic determinants of plasma total homocysteine. *Semin Vasc Med* 5: 98–109.
7. **Refsum H, Ueland PM, Nygard O, Vollset SE** (1998) Homocysteine and cardiovascular disease. *Annu Rev Med* 49: 31–62.
8. **Hubmacher D, Tiedemann K, Reinhardt DP** (2006) Fibrillins: from biogenesis of microfibrils to signaling functions. *Curr Top Dev Biol* 75: 93–123.
9. **Kielty CM, Sherratt MJ, Marson A, Baldock C** (2005) Fibrillin microfibrils. *Adv Protein Chem* 70: 405–436.
10. **Perla-Kajan J, Twardowski T, Jakubowski H** (2007) Mechanisms of homocysteine toxicity in humans. *Amino Acids* 32: 561–572.
11. **Hubmacher D, Cirulis JT, Miao M, Keeley FW, Reinhardt DP** (2010) Functional consequences of homocysteinylation of the elastic fiber proteins fibrillin-1 and tropoelastin. *J Biol Chem* 285: 1188–1198.
12. **Lawrence de Koning AB, Werstuck GH, Zhou J, Austin RC** (2003) Hyperhomocysteinemia and its role in the development of atherosclerosis. *Clinical Biochemistry* 36: 431–441.
13. **Spence JD, Bang H, Chambless LE, Stampfer MJ** (2005) Vitamin Intervention For Stroke Prevention trial: an efficacy analysis. *Stroke* 36: 2404–2409.
14. **Dodds L, Fell DB, Dooley KC, Armson BA, Allen AC, et al.** (2008) Effect of homocysteine concentration in early pregnancy on gestational hypertensive disorders and other pregnancy outcomes. *Clin Chem* 54: 326–334.
15. **Mattson MP, Shea TB** (2003) Folate and homocysteine metabolism in neural plasticity and neurodegenerative disorders. *Trends Neurosci* 26: 137–146.
16. **Obeid R, Herrmann W** (2006) Mechanisms of homocysteine neurotoxicity in neurodegenerative diseases with special reference to dementia. *FEBS Lett* 580: 2994–3005.
17. **Seshadri S** (2006) Elevated plasma homocysteine levels: risk factor or risk marker for the development of dementia and Alzheimer's disease? *J Alzheimers Dis* 9: 393–398.
18. **Chwatko G, Jakubowski H** (2005) Urinary excretion of homocysteine-thiolactone in humans. *Clin Chem* 51: 408–415.
19. **Jakubowski H** (2000) Calcium-dependent human serum homocysteine thiolactone hydrolase. A protective mechanism against protein N-homocysteinylation. *J Biol Chem* 275: 3957–3962.

20. **Zimny J, Sikora M, Guranowski A, Jakubowski H** (2006) Protective mechanisms against homocysteine toxicity: the role of bleomycin hydrolase. *J Biol Chem* 281: 22485–22492.
21. **Jakubowski H** (1997) Metabolism of homocysteine thiolactone in human cell cultures. Possible mechanism for pathological consequences of elevated homocysteine levels. *J Biol Chem* 272: 1935–1942.
22. **Jakubowski H** (1999) Protein homocysteinylation: possible mechanism underlying pathological consequences of elevated homocysteine levels. *FASEB J* 13: 2277–2283.
23. **Jakubowski H** (2000) Homocysteine thiolactone: metabolic origin and protein homocysteinylation in humans. *J Nutr* 130: 377S–381S.
24. **Jakubowski H, Zhang L, Bardeguet A, Aviv A** (2000) Homocysteine thiolactone and protein homocysteinylation in human endothelial cells: implications for atherosclerosis. *Circ Res* 87: 45–51.
25. **Jakubowski H, Goldman E** (1993) Synthesis of homocysteine thiolactone by methionyl-tRNA synthetase in cultured mammalian cells. *FEBS Lett* 317: 237–240.
26. **Jakubowski H** (2003) Homocysteine-thiolactone and S-nitroso-homocysteine mediate incorporation of homocysteine into protein in humans. *Clin Chem Lab Med* 41: 1462–1466.
27. **Jakubowski H** (2004) Molecular basis of homocysteine toxicity in humans. *Cell Mol Life Sci* 61: 470–487.
28. **Jalili S, Yousefi R, Papari MM, Moosavi-Movahedi AA** (2011) Effect of homocysteine thiolactone on structure and aggregation propensity of bovine pancreatic insulin. *Protein J* 30: 299–307.
29. **Khazaei S, Yousefi R, Alavian-Mehr MM** (2012) Aggregation and fibrillation of eye lens crystallins by homocysteinylation; implication in the eye pathological disorders. *Protein J* 31: 717–727.
30. **Paoli P, Sbrana F, Tiribilli B, Caselli A, Pantera B, et al.** (2010) Protein N-homocysteinylation induces the formation of toxic amyloid-like protofibrils. *J Mol Biol* 400: 889–907.
31. **Stroylova YY, Chobert JM, Muronetz VI, Jakubowski H, Haertle T** (2012) N-homocysteinylation of ovine prion protein induces amyloid-like transformation. *Arch Biochem Biophys* 526: 29–37.
32. **Stroylova YY, Zimny J, Yousefi R, Chobert JM, Jakubowski H, et al.** (2011) Aggregation and structural changes of alpha(S1)-, beta- and kappa-caseins induced by homocysteinylation. *Biochim Biophys Acta* 1814: 1234–1245.
33. **Jakubowski H** (2002) Homocysteine is a protein amino acid in humans: implications for homocysteine-linked disease. *J Biol Chem* 277: 30425–30428.
34. **Hamaguchi K, Kurono A** (1968) Structure of muramidase (lysozyme). I. The effect of guanidine hydrochloride on muramidase. *J Biochem* 54: 111–122.
35. **Bigelow CC** (1960) Difference spectra of ribonuclease and two ribonuclease derivatives. *C R Trav Lab Carlsberg* 31: 305–324.
36. **Sugai S, Yashiro H, Nitta K** (1973) Equilibrium and kinetics of the unfolding of alpha-lactalbumin by guanidine hydrochloride. *Biochim Biophys Acta* 328: 35–41.
37. **Thorn DC, Meehan S, Sunde M, Rekas A, Gras SI, et al.** (2005) Amyloid fibril formation by bovine milk kappa-casein, and its inhibition by the molecular chaperones alphaS and beta-casein. *Biochemistry* 44: 17027–17036.
38. **Yazdanparast R, Khodarahmi R, Soori E** (2005) Comparative studies of the artificial chaperone-assisted refolding of thermally denatured bovine carbonic anhydrase using different capturing ionic detergents and beta-cyclodextrin. *Arch Biochem Biophys* 437: 178–185.
39. **Pace CN** (1986) Determination and analysis of urea and guanidine hydrochloride denaturation curves. *Methods Enzymol* 131: 266–280.
40. **Ellman GL** (1959) Tissue sulfhydryl groups. *Arch Biochem Biophys* 82: 70–77.
41. **Yang JT, Wu CS, Martinez HM** (1986) Calculation of protein conformation from circular dichroism. *Methods Enzymol* 130: 208–269.
42. **Maurel C, Westmoreland D** (1976) Catalytic implications of electrostatic potential: The lytic activity of lysozyme as a model. *J Mol Biol* 102: 253–264.

43. **Crook EM, Mathias AP, Rabin BR** (1960) Spectrophotometric assay of bovine pancreatic ribonuclease by the use of cytidine 2':3'-phosphate. *Biochem J* 74: 234–238.
44. **Sinha A, Yadav S, Ahmad R, Ahmad F** (2000) A possible origin of differences between calorimetric and equilibrium estimates of stability parameters of proteins. *Biochem J* 345 Pt 3: 711–717.
45. **Chwatko G, Jakubowski H** (2005) The determination of homocysteine-thiolactone in human plasma. *Anal Biochem* 337: 271–277.
46. **Sikora M, Marczak L, Kubalska J, Graban A, Jakubowski H** (2014) Identification of N-homocysteinylation sites in plasma proteins. *Amino Acids* 46: 235–244.
47. **Dudman NP, Hicks C, Lynch JF, Wilcken DE, Wang J** (1991) Homocysteine thiolactone disposal by human arterial endothelial cells and serum in vitro. *Arterioscler Thromb* 11: 663–670.
48. **Arora B, Narayanasamy A, Nirmal J, Halder N, Patnaik S, et al.** (2014) Development and validation of a LC-MS/MS method for homocysteine thiolactone in plasma and evaluation of its stability in plasma samples. *Journal of Chromatography B* 944: 49–54.
49. **Perla-Kajan J, Marczak L, Kajan L, Skowronek P, Twardowski T, et al.** (2007) Modification by homocysteine thiolactone affects redox status of cytochrome C. *Biochemistry* 46: 6225–6231.
50. **Zang T, Dai S, Chen D, Lee BW, Liu S, et al.** (2009) Chemical methods for the detection of protein N-homocysteinylation via selective reactions with aldehydes. *Anal Chem* 81: 9065–9071.
51. **Ferretti G, Bacchetti T, Moroni C, Vignini A, Nanetti L, et al.** (2004) Effect of homocysteinylation of low density lipoproteins on lipid peroxidation of human endothelial cells. *J Cell Biochem* 92: 351–360.
52. **Khodadadi S, Riazi GH, Ahmadian S, Hoveizi E, Karima O, et al.** (2012) Effect of N-homocysteinylation on physicochemical and cytotoxic properties of amyloid beta-peptide. *FEBS Lett* 586: 127–131.
53. **Stühlinger MC, Tsao PS, Her JH, Kimoto M, Balint RF, et al.** (2001) Homocysteine Impairs the Nitric Oxide Synthase Pathway Role of Asymmetric Dimethylarginine. *Circulation* 104: 2569–2575.
54. **Yousefi R, Jalili S, Alavi P, Moosavi-Movahedi AA** (2012) The enhancing effect of homocysteine thiolactone on insulin fibrillation and cytotoxicity of insulin fibril. *Int J Biol Macromol* 51: 291–298.
55. **Glowacki R, Jakubowski H** (2004) Cross-talk between Cys34 and lysine residues in human serum albumin revealed by N-homocysteinylation. *J Biol Chem* 279: 10864–10871.
56. **Topal G, Brunet A, Millanvoye E, Boucher J, Rendu F, et al.** (2004) Homocysteine induces oxidative stress by uncoupling of NO synthase activity through reduction of tetrahydrobiopterin. *Free Radic Biol Med* 36: 1532–1541.
57. **Hong L, Fast W** (2007) Inhibition of Human Dimethylarginine Dimethylaminohydrolase-1 by S-Nitroso-L-homocysteine and Hydrogen Peroxide: Analysis, quantification, and implications for hyperhomocysteinemia. *J Bio Chem* 282: 34684–34692.
58. **Sontag E, Nunbhakdi-Craig V, Sontag JM, Diaz-Arrastia R, Ogris E, et al.** (2007) Protein phosphatase 2A methyltransferase links homocysteine metabolism with tau and amyloid precursor protein regulation. *J Neurosci* 27: 2751–2759.
59. **Karima O, Riazi G, Khodadadi S, Aryapour H, Khalili MA, et al.** (2012) Altered tubulin assembly dynamics with N-homocysteinylation of human 4R/1N tau in vitro. *FEBS Lett* 586: 3914–3919.